Noname manuscript No.
(will be inserted by the editor)

An efficient differential quadrature method for fractional advection-diffusion equation

X. G. Zhu · Y. F. Nie · W. W. Zhang

arXiv:1611.01597v1 [math.NA] 5 Nov 2016

Received: date / Accepted: date

Abstract Using a set of modified cubic trigonometric B-splines as test functions, a new differential quadrature technique is proposed for the 1D and 2D transient advection-diffusion equations of order $\alpha \in (0, 1]$. The weighted coefficients are determined via solving the system of algebraic equations with a strictly diagonally dominant tri-diagonal matrix. Then, the original equation is converted into an ordinary differential system (ODS), which is discretized by a third-order Gorenflo-Mainardi-Moretti-Paradisi (GMMP) scheme in fractional case and by Runge-Kutta Gill's method if $\alpha = 1$. The resulting method is evaluated on four benchmark problems and a concrete simulation of the unsteady propagation of a Gaussian pulse. In comparison with the existent algorithms in open literature, the numerical results finally illustrate its validity and accuracy.

Keywords Differential quadrature method (DQM) · Modified cubic trigonometric B-spline function · Fractional advection-diffusion equation (FADE)

1 Introduction

The differential equations with a fractional derivative serve as superior models in subjects as diverse as astrophysics, chaotic dynamics, fractal network, signal processing, continuum mechanics, turbulent flow and wave propagation [22,27,33,38]. These equations admit the non-local memory effects in mathematical mechanism, thereby filling in a big gap that the classic models can not work well for some of the natural phenomena like anomalous transport. In general, the true closed-form solutions are unavailable to access or even non-existent, so a keen interest has been attracted to design robust algorithm to study them in a numerical perspective.

In this article, we aim to construct an efficient method to solve the advection-diffusion equations:

(I) 1D FADE

$$\frac{\partial^\alpha u(x,t)}{\partial t^\alpha} + \kappa \frac{\partial u(x,t)}{\partial x} - \varepsilon \frac{\partial^2 u(x,t)}{\partial x^2} = f(x,t), \quad (1)$$

with $0 < \alpha \le 1$, $\kappa, \varepsilon \ge 0$, $a \le x \le b$, $t > 0$, and the initial and boundary conditions

$$u(x,0) = \varphi(x), \quad a \le x \le b, \quad (2)$$
$$u(a,t) = g_1(t), \quad u(b,t) = g_2(t), \quad t > 0. \quad (3)$$

(II) 2D FADE

$$\begin{aligned} &\frac{\partial^\alpha u(x,y,t)}{\partial t^\alpha} + \kappa_x \frac{\partial u(x,y,t)}{\partial x} + \kappa_y \frac{\partial u(x,y,t)}{\partial y} \\ &- \varepsilon_x \frac{\partial^2 u(x,y,t)}{\partial x^2} - \varepsilon_y \frac{\partial^2 u(x,y,t)}{\partial y^2} = f(x,y,t), \end{aligned} \quad (4)$$

with $0 < \alpha \le 1$, $\kappa_x, \kappa_y, \varepsilon_x, \varepsilon_y \ge 0$, $(x, y) \in \Omega$, $t > 0$, and the initial and boundary conditions

$$u(x,y,0) = \varphi(x,y), \quad (x,y) \in \Omega, \quad (5)$$
$$u(x,y,t) = g(x,y,t), \quad (x,y) \in \partial\Omega, \quad t > 0, \quad (6)$$

where $\Omega = \{(x, y) : a \le x \le b, c \le y \le d\}$ and $\partial\Omega$ denotes its boundary.

X. G. Zhu · Y. F. Nie · W. W. Zhang
Department of Applied Mathematics, Northwestern Polytechnical University, Xi'an, Shanxi 710129, P. R. China
E-mail: yfnie@nwpu.edu.cn

X. G. Zhu
E-mail: zhuxg590@yeah.net

W. W. Zhang
E-mail: wwzhang@nwpu.edu.cn

In Eqs. (1), (4), the time-fractional derivatives are defined in Caputo sense, i.e.,

$$\frac{\partial^\alpha u(x,t)}{\partial t^\alpha} = \frac{1}{\Gamma(1-\alpha)} \int_0^t \frac{\partial u(x,\xi)}{\partial \xi} \frac{d\xi}{(t-\xi)^\alpha},$$

and $\frac{\partial^\alpha u(x,y,t)}{\partial t^\alpha}$ is an analog of $\frac{\partial^\alpha u(x,t)}{\partial t^\alpha}$, where $\Gamma(\cdot)$ is the Euler's Gamma function. It is noted that Eqs. (1)-(3) and (4)-(6) degenerate to the classic 1D and 2D advection-diffusion equations if $\alpha = 1$ is fixed.

In recent decades, FADE has been a notable subject of intense research. Except for a few analytic solutions, various numerical methods have been done for Eqs. (1)-(3) without advection, covering implicit difference method [42], high-order finite element method (FEM) [15], Legendre wavelets and spectral Galerkin methods [10,18], direct discontinuous Galerkin method [12], quadratic spline collocation method [20], cubic B-spline collocation method (CBCM) [30], orthogonal spline collocation method [37], pseudo-spectral method [7], high-order compact difference method [14], implicit RBF meshless method [19], nonpolynomial and polynomial spline methods [11]. In [3,5,29,41], the algorithms based on shifted fractional Jacobi polynomials, Sinc functions and shifted Legendre polynomials, Haar wavelets and the third kind Chebyshev wavelets functions were well developed via the integral operational matrix or collocation strategy for Eqs. (1)-(3) with variable coefficients. The Gegenbauer polynomial spectral collocation method was proposed in [13] for the same type equation and a Sinc-Haar collocation method can be found in [26]. Uddin and Haq considered a radial basis interpolation approach for FADE [35]. Cui established a high-order compact exponential difference scheme [6]. Razminia et al. proposed a DQM for fractional diffusion equation by using lagrange interpolation basis as test functions [28]. Shirzadi et al. solved a 2D FADE with a reaction term via a local Petrov-Galerkin meshless method [32]. Gao and Sun derived two different three-point combined compact ADI schemes for Eqs. (4)-(6) [8], both of which own high accuracy.

The trigonometric B-splines are a class of piecewise-defined functions constructed from algebraic trigonometric spaces, which have got recognition since 1964. They are preferred to the familiar polynomial B-splines since they often yield less errors when served as basis functions in interpolation theory. Nevertheless, using those scaling functions to set up numerical algorithm is in its infancy and the related works are still limited [1, 24]. In this study, a new DQM for the integer and fractional advection-diffusion equation is proposed with its weighted coefficients calculated based on a set of modified cubic trigonometric B-spline (CTB) basis. A third-order GMMP scheme is used to deal with the resulting ODSs if $\alpha \in (0,1)$, whereas Runge-Kutta Gill's method is employed when its power is 1. The technique in presence is straight forward to apply and highly accurate; five numerical tests are provided to confirm its capability as compared with some already known results.

The remainder is organized as follows. In Section 2, we outline some basic definitions and the modified CTB basis functions that are very useful hereinafter. In Section 3, how to determine the weighted coefficients based on those basis functions is detailedly investigated. Section 4 constructs a new DQM for solving Eqs. (1)-(3) and Eqs. (4)-(6). A couple of numerical examples are included in Section 5, which manifest the effectiveness of our method. The last section gives a conclusion.

2 Preliminaries

Let $M, N \in \mathbb{Z}^+$ and a time-space lattice be

$$\Omega_\tau = \{t_n : t_n = n\tau,\ 0 \le n \le N\},$$
$$\Omega_h = \{x_i : x_i = a + ih,\ 0 \le i \le M\},$$

with $\tau = T/N$, $h = (b-a)/M$ on $(0,T] \times [a,b]$. Then, some auxiliary results are introduced for preliminaries.

2.1 GMMP scheme for Caputo derivative

Given a good enough $f(x,t)$, the formulas

$${}_0^C D_t^\alpha f(x,t) = \frac{1}{\Gamma(m-\alpha)} \int_0^t \frac{\partial^m f(x,\xi)}{\partial \xi^m} \frac{d\xi}{(t-\xi)^{1+\alpha-m}},$$
$${}_0^{RL} D_t^\alpha f(x,t) = \frac{1}{\Gamma(m-\alpha)} \frac{\partial^m}{\partial t^m} \int_0^t \frac{f(x,\xi)d\xi}{(t-\xi)^{1+\alpha-m}},$$

define the α-th Caputo and Riemann-Liouville derivatives, respectively, where $m-1 < \alpha < m$, $m \in \mathbb{Z}^+$.

The two frequently-used fractional derivatives are equivalent with exactness to an additive factor, i.e.,

$${}_0^C D_t^\alpha f(x,t) = {}_0^{RL} D_t^\alpha f(x,t) - \sum_{l=0}^{m-1} \frac{f^{(l)}(x,0) t^{l-\alpha}}{\Gamma(l+1-\alpha)}; \tag{7}$$

see [17,27] for references. Utilizing ${}_0^{RL} D_t^\alpha t^l = \frac{\Gamma(l+1)t^{l-\alpha}}{\Gamma(l+1-\alpha)}$ and a valid scheme to discretize the right side of Eq. (7), a GMMP scheme for Caputo derivative reads [9,23]

$$\begin{aligned} {}_0^C D_t^\alpha f(x,t_n) \cong & \frac{1}{\tau^\alpha} \sum_{k=0}^{n} \omega_k^\alpha f(x,t_{n-k}) \\ & - \frac{1}{\tau^\alpha} \sum_{l=0}^{m-1} \sum_{k=0}^{n} \frac{\omega_k^\alpha f^{(l)}(x,0) t_{n-k}^l}{l!}. \end{aligned} \tag{8}$$

Here, we choose the coefficients ω_k^α [4]:

$$\omega_k^\alpha = \left(\frac{11}{6}\right)^\alpha \sum_{p=0}^{k}\sum_{q=0}^{p} \mu^q \overline{\mu}^{p-q} l_q^\alpha l_{p-q}^\alpha l_{k-p}^\alpha, \quad k \geq 0,$$

with $\mu = \frac{4}{7+\sqrt{39}\mathrm{i}}$, $\overline{\mu} = \frac{4}{7-\sqrt{39}\mathrm{i}}$, $\mathrm{i} = \sqrt{-1}$, and

$$l_0^\alpha = 1, \quad l_k^\alpha = \left(1 - \frac{\alpha+1}{k}\right) l_{k-1}^\alpha, \quad k \geq 1,$$

in which case, the truncated error fulfilling $\mathscr{R}_\tau = \mathscr{O}(\tau^3)$. Reset $0 < \alpha < 1$, (8) thus turns into

$$\begin{aligned} {}_0^C D_t^\alpha f(x,t_n) = \frac{1}{\tau^\alpha}\sum_{k=0}^{n-1} \omega_k^\alpha f(x,t_{n-k}) \\ - \frac{1}{\tau^\alpha}\sum_{k=0}^{n-1} \omega_k^\alpha f(x,0) + \mathscr{R}_\tau. \end{aligned} \tag{9}$$

We note that Eq. (9) do not recover to the classic four-point backward difference scheme when $\alpha = 1$ though its coefficients vanish apart from ω_0^1, ω_1^1, ω_2^1 and ω_3^1.

2.2 Trigonometric spline functions

Let $x_{-i} = a - ih$, $x_{M+i} = b + ih$, $i = 1,2,3$ be the six ghost knots outside $[a,b]$. Then the desirable CTB basis functions $\{CTB_m(x)\}_{m=-1}^{M+1}$ are defined as [24,36]

$$CTB_m(x) = \frac{1}{\chi}\begin{cases} \phi_1(x), & x \in [x_{m-2}, x_{m-1}) \\ \phi_2(x), & x \in [x_{m-1}, x_m) \\ \phi_3(x), & x \in [x_m, x_{m+1}) \\ \phi_4(x), & x \in [x_{m+1}, x_{m+2}) \\ 0, & \text{otherwise} \end{cases}$$

where

$$\begin{aligned} \phi_1(x) &= p^3(x_{m-2}), \\ \phi_2(x) &= q(x_{m+2})p^2(x_{m-1}) + p^2(x_{m-2})q(x_m) \\ &\quad + p(x_{m-2})p(x_{m-1})q(x_{m+1}), \\ \phi_3(x) &= p(x_{m-2})q^2(x_{m+1}) + q^2(x_{m+2})p(x_m) \\ &\quad + p(x_{m-1})q(x_{m+1})q(x_{m+2}), \\ \phi_4(x) &= q^3(x_{m+2}), \end{aligned}$$

with the notations

$$\begin{aligned} p(x_m) &= \sin\left(\frac{x - x_m}{2}\right), \\ q(x_m) &= \sin\left(\frac{x_m - x}{2}\right), \\ \chi &= \sin\left(\frac{h}{2}\right)\sin(h)\sin\left(\frac{3h}{2}\right). \end{aligned}$$

The values of $CTB_m(x)$ at each knot are given by

$$CTB_m(x_i) = \begin{cases} \sin^2\left(\frac{h}{2}\right)\csc(h)\csc\left(\frac{3h}{2}\right), & i = m \pm 1 \\ \frac{2}{1+2\cos(h)}, & i = m \\ 0, \quad \text{otherwise} \end{cases} \tag{10}$$

and the values of $CTB'_m(x)$ at each knot are given by

$$CTB'_m(x_i) = \begin{cases} \frac{3}{4}\csc\left(\frac{3h}{2}\right), & i = m-1 \\ -\frac{3}{4}\csc\left(\frac{3h}{2}\right), & i = m+1 \\ 0. \quad \text{otherwise} \end{cases} \tag{11}$$

The CTB basis $\{CTB_m(x)\}_{m=-1}^{M+1}$ are locally compact and twice continuously differentiable on $[a,b]$. Since the knots x_{-1}, x_{M+1} lie beyond $[a,b]$ and the weights in relation to the B-splines $CTB_{-1}(x)$, $CTB_{M+1}(x)$ do not participate in practical computation, hereunder, we modify the CTB basis functions in the following way

$$\begin{cases} MTB_0(x) = CTB_0(x) + 2CTB_{-1}(x), \\ MTB_1(x) = CTB_1(x) - CTB_{-1}(x), \\ MTB_m(x) = CTB_m(x), \quad m = 2,3,\ldots,M-2, \\ MTB_{M-1}(x) = CTB_{M-1}(x) - CTB_{M+1}(x), \\ MTB_M(x) = CTB_M(x) + 2CTB_{M+1}(x), \end{cases} \tag{12}$$

such that a diagonally dominant tri-diagonal algebraic system will be generated after discretization on a uniform grid as Ω_h. $\{MTB_m(x)\}_{m=0}^{M}$ are also linear independent and form a family of basis functions on $[a,b]$.

3 The calculation of weighted coefficients

On a 2D domain $[a,b]\times[c,d]$, letting $M_x, M_y \in \mathbb{Z}^+$, we add a spatial lattice with equally spaced points with spacing of $h_x = (b-a)/M_x$ in x-axis and $h_y = (d-c)/M_y$ in y-axis, i.e.,

$$\begin{aligned} \Omega_x &= \{x_i : x_i = a + ih_x,\ 0 \leq i \leq M_x\}, \\ \Omega_y &= \{y_j : y_j = c + jh_y,\ 0 \leq j \leq M_y\}. \end{aligned}$$

DQM is understood as a numerical technique for finding the approximate solution to differential equation that reduces the original equation to those of solving a system of algebraic or ordinary differential equations via replacing the partial derivatives at certain grid points by a representative weighted combination of functional values [2]. The key procedure of such method lies in the determination of its weights and the selection of the test functions whose derivative values are explicit

at the prescribed discrete grid points. As requested, we let

$$\frac{\partial^s u(x_i,t)}{\partial x^s} = \sum_{j=0}^{M} a_{ij}^{(s)} u(x_j,t), \quad 0 \le i \le M, \tag{13}$$

while for 2D problems, we let

$$\frac{\partial^s u(x_i,y_j,t)}{\partial x^s} = \sum_{m=0}^{M_x} a_{im}^{(s)} u(x_m,y_j,t), \tag{14}$$

$$\frac{\partial^s u(x_i,y_j,t)}{\partial y^s} = \sum_{m=0}^{M_y} b_{jm}^{(s)} u(x_i,y_m,t), \tag{15}$$

where $s \in \mathbb{Z}^+$, $0 \le i \le M_x$, $0 \le j \le M_y$ and $a_{ij}^{(s)}$, $a_{im}^{(s)}$, $b_{jm}^{(s)}$ are the weighted coefficients allowing us to approximate the s-th derivatives or partial derivatives at the given grid points very accurately.

In the sequel, we apply the modified CTB basis to calculate these 1D, 2D unknown weights. Putting $s=1$ and inserting $\{MTB_m(x)\}_{m=0}^{M}$ into Eq. (13), we have

$$\frac{\partial MTB_m(x_i)}{\partial x} = \sum_{j=0}^{M} a_{ij}^{(1)} MTB_m(x_j), \quad 0 \le i,m \le M,$$

with the weighted coefficients of the first-order derivative $a_{ij}^{(1)}$, $0 \le i,j \le M$, yet to be determined. In view of (12) and the properties (10)-(11), the above equations can be written in the matrix-vector form

$$\begin{cases} \mathbf{A}\mathbf{a}_0^{(1)} = \mathbf{Z}_0, \\ \mathbf{A}\mathbf{a}_1^{(1)} = \mathbf{Z}_1, \\ \quad \vdots \\ \mathbf{A}\mathbf{a}_M^{(1)} = \mathbf{Z}_M, \end{cases} \tag{16}$$

where $\mathbf{A}$ is the $(M+1)\times(M+1)$ coefficient matrix

$$\mathbf{A} = \begin{pmatrix} A_0+2A_1 & A_1 & & & & \\ 0 & A_0 & A_1 & & & \\ & A_1 & A_0 & A_1 & & \\ & & \ddots & \ddots & \ddots & \\ & & & A_1 & A_0 & 0 \\ & & & & A_1 & A_0+2A_1 \end{pmatrix},$$

$$A_0 = \frac{2}{1+2\cos(h)}, \quad A_1 = \sin^2\left(\frac{h}{2}\right)\csc(h)\csc\left(\frac{3h}{2}\right),$$

$\mathbf{a}_k^{(1)}$, $0 \le k \le M$, are the weighted coefficient vectors at x_k, i.e., $\mathbf{a}_k^{(1)} = [a_{k0}^{(1)}, a_{k1}^{(1)}, \ldots, a_{kM}^{(1)}]^{\mathrm{T}}$, and the right-side vectors $\mathbf{Z}_k$ at x_k, $0 \le k \le M$, are as follows

$$\mathbf{Z}_0 = \begin{pmatrix} -2z \\ 2z \\ 0 \\ 0 \\ \vdots \\ 0 \\ 0 \end{pmatrix}, \quad \mathbf{Z}_1 = \begin{pmatrix} -z \\ 0 \\ z \\ 0 \\ \vdots \\ 0 \\ 0 \end{pmatrix}, \cdots,$$

$$\mathbf{Z}_{M-1} = \begin{pmatrix} 0 \\ 0 \\ \vdots \\ 0 \\ -z \\ 0 \\ z \end{pmatrix}, \quad \mathbf{Z}_M = \begin{pmatrix} 0 \\ 0 \\ \vdots \\ 0 \\ 0 \\ -2z \\ 2z \end{pmatrix},$$

with $z = \frac{3}{4}\csc\left(\frac{3h}{2}\right)$, respectively. Thus, $a_{ij}^{(1)}$ are obtained by solving Eqs. (16). The weighted coefficients $a_{ij}^{(s)}$, $s \ge 2$, corresponding to high-order derivatives can be found in a recursive style [34], i.e.,

$$a_{ij}^{(s)} = s\left(a_{ii}^{(s-1)} a_{ij}^{(1)} - \frac{a_{ij}^{(s-1)}}{x_i - x_j}\right), \quad i \ne j,\ 0 \le i \le M,$$

$$a_{ii}^{(s)} = -\sum_{j=0, j\ne i}^{M} a_{ij}^{(s)}, \quad i = j.$$

Proceeding as above via replacing Ω_h by Ω_x, Ω_y leads in a straightforward way to a 2D generalization to acquire $a_{im}^{(1)}$, $b_{jm}^{(1)}$ of the partial derivatives with regard to x, y, and by them, the following relations are further applied, i.e.,

$$a_{im}^{(s)} = s\left(a_{ii}^{(s-1)} a_{im}^{(1)} - \frac{a_{im}^{(s-1)}}{x_i - x_m}\right), \quad i \ne m,\ 0 \le i \le M,$$

$$a_{ii}^{(s)} = -\sum_{m=0, m\ne i}^{M_x} a_{im}^{(s)}, \quad i = m,$$

$$b_{jm}^{(s)} = s\left(b_{jj}^{(s-1)} b_{jm}^{(1)} - \frac{b_{jm}^{(s-1)}}{y_j - y_m}\right), \quad j \ne m,\ 0 \le j \le M,$$

$$b_{jj}^{(s)} = -\sum_{m=0, m\ne j}^{M_y} b_{jm}^{(s)}, \quad j = m,$$

to calculate $a_{im}^{(s)}$, $b_{jm}^{(s)}$, $s \ge 2$. Due to A_0, $A_1 > 0$, $0 < h < 1$, $0 < h_x$, $h_y < 1$, $A_0 > 2A_1$, we then know that $\mathbf{A}$ is a strictly diagonally dominant matrix. Hence, Thomas algorithm is employed to tackle the algebraic equations as Eqs. (16) that would greatly economize the memory and computing cost in practise.

4 Description of CTB based DQM

In this part, we construct a modified CTB based DQM (MCTB-DQM) for Eqs. (1)-(3) and Eqs. (4)-(6). Let $s = 1, 2$. Inserting the weighted sums (13), (14)-(15) into the equations under consideration, we have

$$\frac{\partial^\alpha u(x_i,t)}{\partial t^\alpha} + \kappa \sum_{j=0}^{M} a_{ij}^{(1)} u(x_j,t) - \varepsilon \sum_{j=0}^{M} a_{ij}^{(2)} u(x_j,t) = f(x_i,t),$$

with $i = 0, 1, \cdots, M$, and

$$\frac{\partial^\alpha u(x_i,y_j,t)}{\partial t^\alpha} + \kappa_x \sum_{m=0}^{M_x} a_{im}^{(1)} u(x_m,y_j,t) + \kappa_y \sum_{m=0}^{M_y} b_{jm}^{(1)} u(x_i,y_m,t)$$
$$- \varepsilon_x \sum_{m=0}^{M_x} a_{im}^{(2)} u(x_m,y_j,t) - \varepsilon_y \sum_{m=0}^{M_y} b_{jm}^{(2)} u(x_i,y_m,t) = f(x_i,y_j,t),$$

with $i = 0, 1, \cdots, M_x$, $j = 0, 1, \cdots, M_y$, which are indeed a family of α-th ODSs involving $\alpha \in (0, 1)$ and $\alpha = 1$ as two cases. In what follows, we denote

$$u_i^n = u(x_i,t_n), \quad g_1^n = g_1(t_n), \quad g_2^n = g_2(t_n),$$
$$u_{ij}^n = u(x_i,y_j,t_n), \quad g_{ij}^n = g(x_i,y_j,t_n),$$
$$f_i^n = f(x_i,t_n), \quad f_{ij}^n = f(x_i,y_j,t_n),$$

where $n = 0, 1, \cdots, N$, for the ease of exposition.

4.1 The case of fractional order

Discretizing the ODSs above by GMMP scheme (9) and imposing boundary restriction on them, we obtain

$$\begin{cases} \omega_0^\alpha U_i^n + \kappa\tau^\alpha \sum_{j=1}^{M-1} a_{ij}^{(1)} U_j^n - \varepsilon\tau^\alpha \sum_{j=1}^{M-1} a_{ij}^{(2)} U_j^n \\ \quad = -\sum_{k=1}^{n-1} \omega_k^\alpha U_i^{n-k} + \sum_{k=0}^{n-1} \omega_k^\alpha U_i^0 + \tau^\alpha G_i^n, \end{cases} \tag{17}$$

with $i = 1, 2, \cdots, M-1$ and

$$G_i^n = f_i^n - \kappa\big(a_{i0}^{(1)} g_1^n + a_{iM}^{(1)} g_2^n\big) + \varepsilon\big(a_{i0}^{(2)} g_1^n + a_{iM}^{(2)} g_2^n\big),$$

for Eqs. (1)-(3), and the following scheme

$$\begin{cases} \omega_0^\alpha U_{ij}^n + \kappa_x\tau^\alpha \sum_{m=1}^{M_x-1} a_{im}^{(1)} U_{mj}^n + \kappa_y\tau^\alpha \sum_{m=1}^{M_y-1} b_{jm}^{(1)} U_{im}^n \\ \quad - \varepsilon_x\tau^\alpha \sum_{m=1}^{M_x-1} a_{im}^{(2)} U_{mj}^n - \varepsilon_y\tau^\alpha \sum_{m=1}^{M_y-1} b_{jm}^{(2)} U_{im}^n \\ \quad = -\sum_{k=1}^{n-1} \omega_k^\alpha U_{ij}^{n-k} + \sum_{k=0}^{n-1} \omega_k^\alpha U_{ij}^0 + \tau^\alpha G_{ij}^n, \end{cases} \tag{18}$$

with $i = 1, 2, \cdots, M_x - 1$, $j = 1, 2, \cdots, M_y - 1$, and

$$G_{ij}^n = f_{ij}^n - \kappa_x\big(a_{i0}^{(1)} g_{0j}^n + a_{iM_x}^{(1)} g_{M_x j}^n\big) - \kappa_y\big(b_{j0}^{(1)} g_{i0}^n + b_{jM_y}^{(1)} g_{iM_y}^n\big)$$
$$+ \varepsilon_x\big(a_{i0}^{(2)} g_{0j}^n + a_{iM_x}^{(2)} g_{M_x j}^n\big) + \varepsilon_y\big(b_{j0}^{(2)} g_{i0}^n + b_{jM_y}^{(2)} g_{iM_y}^n\big),$$

for Eqs. (4)-(6). As a result, the solutions can be got by performing the procedures defined in Eqs. (17), (18) over and over until all the time levels are reached.

4.2 The case of integer order

When $\alpha = 1$, despite $\omega_0^1 = 1.8333$, $\omega_1^1 = -3$, $\omega_2^1 = 1.5$, $\omega_3^1 = -0.3333$, being the coefficients of the four-point backward difference scheme, the second terms on the right sides of Eqs. (17), (18) lose their meanings. In view of this and to make the algorithm to be more cost-effective, we use Runge-Kutta Gill's method to treat those ODSs instead, which is explicit and fourth-order convergent. Rearrange the ODSs in a unified form

$$\frac{\partial \mathbf{u}}{\partial t} = \mathbf{F}(\mathbf{u}),$$

then the DQM is constructed as follow

$$\begin{aligned} &\mathbf{U}^n = \mathbf{U}^{n-1} + \frac{1}{6}\Big[K_1 + (2-\sqrt{2})K_2 + (2+\sqrt{2})K_3 + K_4\Big], \\ &K_1 = \tau\mathbf{F}(t_{n-1}, \mathbf{U}^{n-1}), \\ &K_2 = \tau\mathbf{F}\Big(t_{n-1} + \frac{\tau}{2}, \mathbf{U}^{n-1} + \frac{K_1}{2}\Big), \\ &K_3 = \tau\mathbf{F}\Big(t_{n-1} + \frac{\tau}{2}, \mathbf{U}^{n-1} + \frac{\sqrt{2}-1}{2}K_1 + \frac{2-\sqrt{2}}{2}K_2\Big), \\ &K_4 = \tau\mathbf{F}\Big(t_{n-1} + \tau, \mathbf{U}^{n-1} - \frac{\sqrt{2}}{2}K_2 + \frac{2+\sqrt{2}}{2}K_3\Big), \end{aligned} \tag{19}$$

where $\mathbf{u}$, $\mathbf{U}^n$, $n = 1, 2, \ldots, N$, are the unknown vectors and $\mathbf{F}(\cdot)$ is an appropriate matrix-vector system that contains $a_{ij}^{(s)}$ or $a_{im}^{(s)}$, $b_{jm}^{(s)}$, $s = 1, 2$, as its elements.

5 Illustrative examples

In this section, a couple of numerical examples are carried out to gauge the actual performance of our new MCTB-DQM. In order to check its accuracy, we compute the error by using the following norms

$$e_\infty(M) \cong \max_i \Big|u_i^n - U_i^n\Big|,$$
$$e_2(M) \cong \sqrt{\frac{1}{M}\sum_{i=1}^{M-1}\Big|u_i^n - U_i^n\Big|^2},$$
$$e_N(M) \cong \sqrt{\sum_{i=1}^{M-1}\Big|u_i^n - U_i^n\Big|^2 \Big/ \sum_{i=1}^{M-1}\Big|U_i^0\Big|^2},$$
$$e_\infty(M_x, M_y) \cong \max_{i,j} \Big|u_{ij}^n - U_{ij}^n\Big|,$$
$$e_2(M_x, M_y) \cong \sqrt{\frac{1}{M_x M_y}\sum_{i=1}^{M_x-1}\sum_{j=1}^{M_y-1}\Big|u_{ij}^n - U_{ij}^n\Big|^2},$$

where $e_N(M)$ is termed by a normalized L_2-norm. The obtained results are comparatively discussed with the potential numerical results available in the literature.

Example 6.1. Let $\kappa = 1$, $\varepsilon = 2$; the Eqs. (1)-(3) with $\varphi(x) = \exp(x)$, $g_1(t) = E(t^\alpha)$, $g_2(t) = eE(t^\alpha)$ and homogeneous forcing term are considered on $[0, 1]$, where $E(t^\alpha)$ is the well-known *Mittag-Leffler function*

$$E_\alpha(z) = \sum_{k=0}^{\infty} \frac{z^k}{\Gamma(\alpha k + 1)}, \quad 0 < \alpha < 1.$$

It is verified that its solution is $u(x, t) = \exp(x)E(t^\alpha)$. Table 1 shows that MCTB-DQM is stable and well convergent at $t = 1$ for various α and $\tau = 1.0 \times 10^{-2}$; the convergent rate is shortly written as "Cov. rate".

Example 6.2. In this test, we solve a diffusion equation on $[0, 1]$ with $\varepsilon = 1$, $\varphi(x) = 4x(1 - x)$, zero boundary condition and right side. Its true solution has the form

$$u(x, t) = \frac{16}{\pi^3} \sum_{k=1}^{\infty} \frac{1}{k^3} E_\alpha(-k^2\pi^2 t^\alpha)(1 - (-1)^k) \sin(k\pi x).$$

For comparison of the numerical results given by FDS-D I, FDS-D II [39] and the semi-discrete FEM [16], we choose the same time stepsize $\tau = 1.0 \times 10^{-4}$. Letting $\alpha = 0.1$, 0.5 and 0.95, the corresponding results of these four methods at $t = 1$ are tabulated side by side in Table 2, from which, we conclude that MCTB-DQM is accurate and produces very small errors as the other three methods as the grid number M increases.

Example 6.3. Let $\kappa = 0$, $\varepsilon = 1$; we solve Eqs. (1)-(3) with homogeneous initial and boundary values, and

$$f(x, t) = \frac{2t^{2-\alpha} \sin(2\pi x)}{\Gamma(3 - \alpha)} + 4\pi^2 t^2 \sin(2\pi x),$$

on $[0, 1]$. The ture solution is $u(x, t) = t^2 \sin(2\pi x)$. The algorithm is first run with $\alpha = 0.8$, $\tau = 2.0 \times 10^{-2}$ and $M = 50$. In Fig. 1, we plot the approximate solution and a point to point error distribution at $t = 1$, where good accuracy is observed. In Table 3, we then report a comparison of $e_2(M)$, $e_\infty(M)$ at $t = 1$ between MCTB-DQM and CBCM [30], when $\alpha = 0.3$. Here, MCTB-DQM uses $\tau = 5.0 \times 10^{-3}$ while CBCM chooses $\tau = 1.25 \times 10^{-3}$. As expected, our approach generates the solutions with a better accuracy than those obtained by CBCM.

Example 6.4. We consider a 2D diffusion equation on $[-1, 1] \times [-1, 1]$ with $\varepsilon_x = \varepsilon_y = 1$, which is referred to by Zhai and Feng as a test of a block-centered finite difference method (BCFDM) on nonuniform grids [40]. The forcing function is specified to enforce

$$u(x, y, t) = (1 + t^2) \tanh(20x) \tanh(20y).$$

Under $\tau = 1.0 \times 10^{-2}$, $M_x = M_y = 60$ and $\alpha = 0.5$, we first plot the approximate solution and a point to point error distribution at $t = 0.5$ in Fig. 2. Then, we compare MCTB-DQM and BCFDM in term of $e_\infty(M_x, M_y)$ at $t = 0.5$ in Table 4. It is obvious that MCTB-DQM produces significantly smaller errors than BCFDM as the grid number increases despite a smaller time stepsize $\tau = 2.5 \times 10^{-3}$ and the nonuniform girds BCFDM adopts; moreover, MCTB-DQM provides more than quadratic rate of convergence for this problem.

Example 6.5. In the last test, we simulate an unsteady propagation of a Gaussian pulse governed by a classic 2D advection-dominated diffusion equation on a square domain $[0, 2] \times [0, 2]$, which has been extensively studied [21,25,31]. The Gaussian pulse solution is expressed as

$$u(x, y, t) = \frac{1}{1 + 4t} \exp\left(-\frac{(x - \kappa_x t - 0.5)^2}{\varepsilon_x(1 + 4t)} - \frac{(y - \kappa_y t - 0.5)^2}{\varepsilon_y(1 + 4t)}\right),$$

and the initial Gaussian pulse and boundary values are taken from the pulse solution. Letting $\kappa_x = \kappa_y = 0.8$, $\varepsilon_x = \varepsilon_y = 0.01$, we display its true solution at $t = 1.25$ with $M_x = M_y = 50$ and the used lattice points on problem domain in Fig. 3, which describe a pulse centred at $(1.5, 1.5)$ with a pulse height of $1/6$. Using the same grid number together with $\tau = 5.0 \times 10^{-3}$, we present the contour plots of the approximate solutions at $t = 0, 0.25, 0.75, 1.25$ created by MCTB-DQM in Fig. 4. As the graph shows, the pulse is initially centred at $(0.5, 0.5)$ with a pulse height of 1, then it moves towards a position centred at $(1.5, 1.5)$; during this process, its width and height appear to be continuously varying as the time goes by. Besides, the last contour plot in Fig. 4 coincides with the true solution plotted in Fig. 3. Retaking $\tau = 2.5 \times 10^{-4}$, $M_x = M_y = 80$, we compare our results and those obtained by using some ADI schemes (PR-ADI, HOC-ADI, PDE-ADI and HPD-ADI) [21] at $t = 1.25$ in Table 5 and better accuracy is admitted.

6 Conclusion

The advection-diffusion equation is a topic of active interest in mathematical physics and the related area of research. In this article, we chiefly focus on a new effective DQM for such equations involving a time derivative of order $(0, 1]$. Its weighted coefficients are calculated by making use of a set of modified CTB basis as test functions. The codes are tested on several benchmark problems and the numerical results have demonstrated that it outperforms some of the previously reported algorithms such as CBCM and BCFDM in term of overall accuracy. The presented approach can be generalized to high-dimensional and the other complex model prob-

Table 1 The numerical results at $t = 1$ with $\tau = 1.0 \times 10^{-2}$ for Example 6.1.

α	M	$e_2(M)$	Cov. rate	$e_\infty(M)$	Cov. rate
0.2	8	1.0412e-02	-	1.4902e-02	-
	16	2.6898e-03	1.9527	3.8827e-03	1.9404
	32	6.6522e-04	2.0156	1.0156e-03	1.9346
	64	1.4842e-04	2.1641	2.5720e-04	1.9814
	128	2.2129e-05	2.7457	6.3504e-05	2.0180
0.5	8	4.4047e-03	-	6.3092e-03	-
	16	1.1394e-03	1.9508	1.6452e-03	1.9392
	32	2.8317e-04	2.0086	4.3121e-04	1.9318
	64	6.4521e-05	2.1338	1.0956e-04	1.9767
	128	1.0443e-05	2.6272	2.7227e-05	2.0086
0.8	8	2.9052e-03	-	4.1559e-03	-
	16	7.5335e-04	1.9473	1.0852e-03	1.9372
	32	1.8911e-04	1.9941	2.8491e-04	1.9294
	64	4.4967e-05	2.0723	7.2683e-05	1.9708
	128	8.7572e-06	2.3603	1.8220e-05	1.9961

Table 2 A comparison of $e_N(M)$ at $t = 1$ with $\tau = 1.0 \times 10^{-4}$ for Example 6.2

α	M	FDS-D I [39]	FDS-D II [39]	FEM [16]	MCTB-DQM
0.1	8	9.98e-04	1.00e-03	5.23e-04	2.7445e-04
	16	2.44e-04	2.53e-04	1.29e-04	3.6823e-05
	32	5.36e-05	6.33e-05	3.21e-05	5.0524e-06
	64	5.89e-06	1.55e-05	8.01e-06	9.6533e-07
	128	6.08e-06	3.62e-06	2.00e-06	4.6423e-07
0.5	8	7.13e-04	7.13e-04	3.37e-04	1.9258e-04
	16	1.79e-04	1.79e-04	8.31e-04	2.6563e-05
	32	4.46e-05	4.44e-05	2.07e-05	4.5588e-06
	64	1.07e-05	1.06e-05	5.17e-06	1.7866e-06
	128	2.23e-06	2.12e-06	1.30e-06	1.4534e-06
0.95	8	1.11e-04	1.11e-04	4.84e-05	2.8976e-05
	16	2.83e-05	2.82e-05	1.21e-05	4.0937e-06
	32	7.09e-06	7.08e-06	3.05e-06	8.7766e-07
	64	1.76e-06	1.75e-06	7.93e-07	4.7682e-07
	128	4.29e-07	4.23e-07	2.32e-07	4.2766e-07

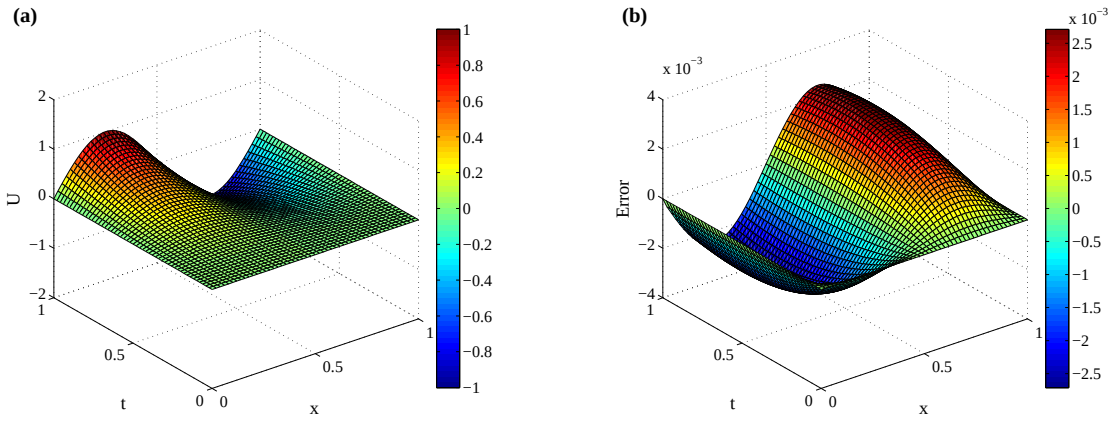

Fig. 1 The approximate solution and error distribution at $t = 1$ with $\alpha = 0.8$ for Example 3

Table 3 A comparison of $e_2(M)$, $e_\infty(M)$ at $t = 1$ with $\alpha = 0.3$ for Example 6.3

M	CBCM [30]		MCTB-DQM	
	$e_2(M)$	$e_\infty(M)$	$e_2(M)$	$e_\infty(M)$
8	3.4134e-02	4.8273e-02	9.4300e-03	1.5762e-02
16	8.7334e-03	1.2351e-02	1.1924e-03	2.1670e-03
32	2.1955e-03	3.1048e-03	1.5040e-04	2.8541e-04
64	5.4957e-04	7.7721e-04	1.8925e-05	3.6701e-05
128	1.3739e-04	1.9430e-04	2.3752e-06	4.6559e-06

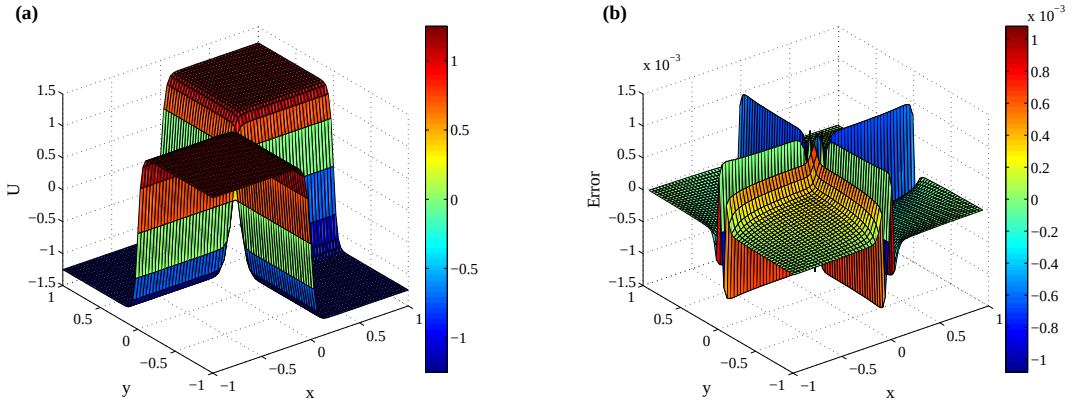

Fig. 2 The approximate solution and error distribution at $t = 0.5$ with $\alpha = 0.5$ for Example 4

Table 4 A comparison of $e_\infty(M_x, M_y)$ at $t = 0.5$ with $\alpha = 0.5$ for Example 6.4

M_x, M_y	BCFDM [40]		MCTB-DQM	
	$e_\infty(M_x, M_y)$	Cov. rate	$e_\infty(M_x, M_y)$	Cov. rate
12	8.75e-02	-	3.3376e-01	-
24	2.73e-02	1.68	4.6331e-03	6.1707
48	8.26e-03	1.73	3.4566e-04	3.7446
96	2.24e-03	1.88	1.8605e-05	4.2156

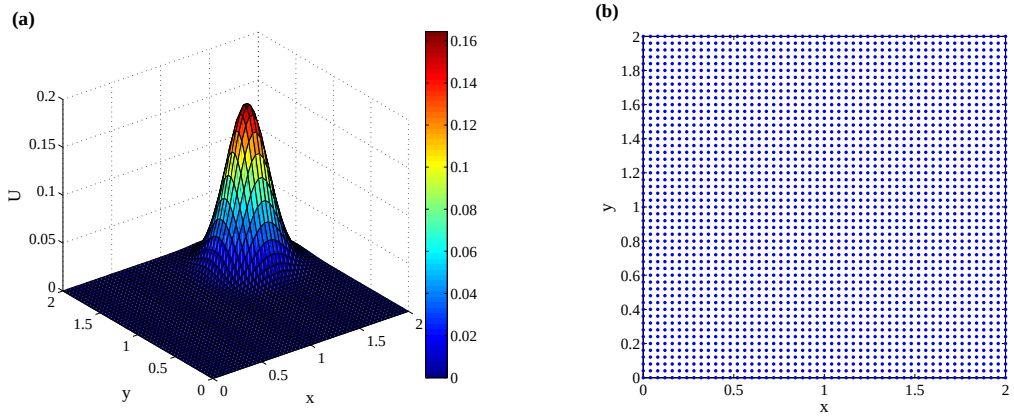

Fig. 3 The true solution at $t = 1.25$ and spatial lattice points for Example 5

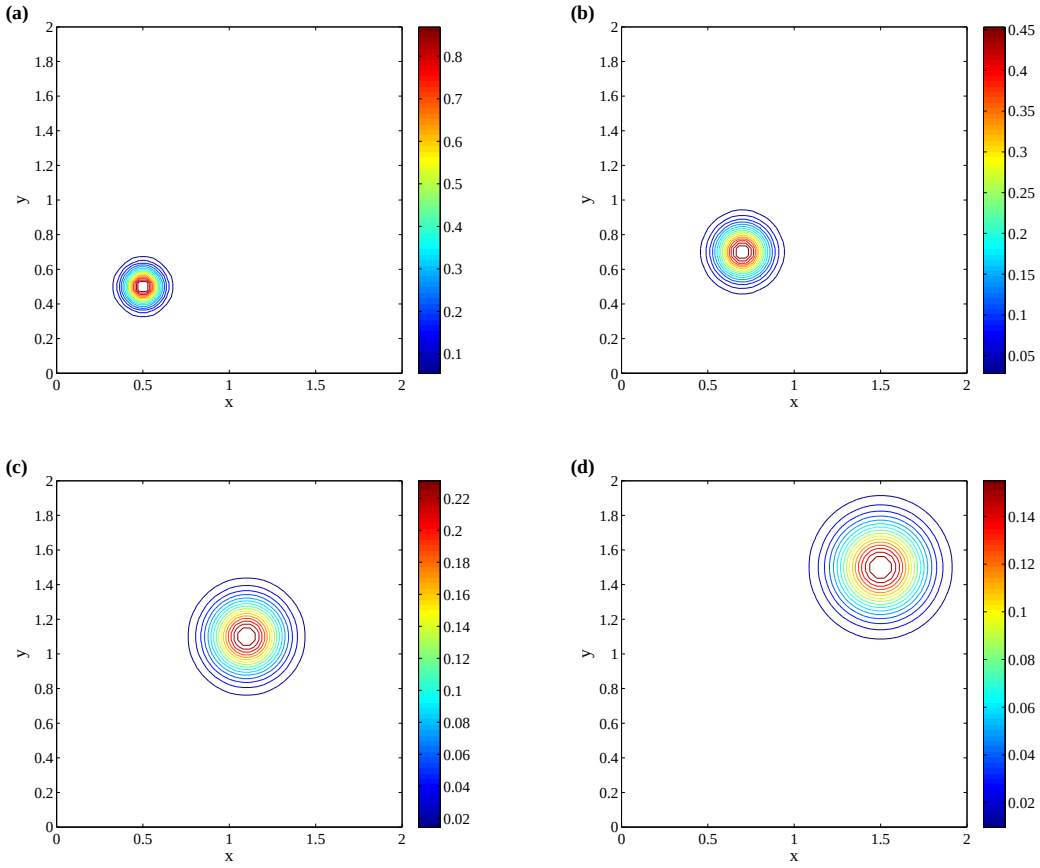

Fig. 4 The contour plots of Gaussian pulse at $t = 0, 0.25, 0.75, 1.25$ with $\tau = 5.0 \times 10^{-3}$ and $M_x = M_y = 50$.

Table 5 The global errors of MCTB-DQM and ADI schemes at $t = 1.25$.

Method	$e_2(M_x, M_y)$	$e_\infty(M_x, M_y)$
PR-ADI [21]	1.11e-03	8.92e-03
HOC-ADI [21]	2.73e-05	2.46e-04
PDE-ADI [21]	2.20e-05	1.71e-04
HPD-ADI [21]	6.38e-05	6.54e-04
MCTB-DQM	5.6737e-06	2.2702e-05

lems arising in material science, structural and fluid mechanics, heat conduction, biomedicine, differential dynamics and so forth. High accuracy, low memory requirement, and the ease of use are its main advantages.

Acknowledgements This research was supported by National Natural Science Foundations of China (No.11471262 and 11501450).

References

1. Abbas, M., Majid, A.A., Ismail, A.I.M., Rashid, A.: The application of cubic trigonometric B-spline to the numerical solution of the hyperbolic problems. Appl. Math. Comput. **239**, 74–88 (2014)
2. Bellman, R., Casti, J.: Differential quadrature and long-term integration. J. Math. Anal. Appl. **34**(2), 235–238 (1971)
3. Bhrawy, A., Zaky, M.: A fractional-order Jacobi Tau method for a class of time-fractional PDEs with variable coefficients. Math. Method Appl. Sci. **39**(7), 1765–1779 (2016)
4. Chen, M.H., Deng, W.H.: Fourth order difference approximations for space Riemann-Liouville derivatives based on weighted and shifted Lubich difference operators. Commun. Comput. Phy. **16**(2), 516–540 (2014)
5. Chen, Y.M., Wu, Y.B., Cui, Y.H., Wang, Z.Z., Jin, D.M.: Wavelet method for a class of fractional convection-diffusion equation with variable coefficients. J. Comput. Sci. **1**(3), 146–149 (2010)
6. Cui, M.R.: A high-order compact exponential scheme for the fractional convection-diffusion equation. J. Comput. Appl. Math. **255**, 404–416 (2014)

7. Esmaeili, S., Garrappa, R.: A pseudo-spectral scheme for the approximate solution of a time-fractional diffusion equation. Int. J. Comput. Math. **92**(5), 980–994 (2015)
8. Gao, G.H., Sun, H.W.: Three-point combined compact alternating direction implicit difference schemes for two-dimensional time-fractional advection-diffusion equations. Commun. Comput. Phy. **17**(2), 487–509 (2015)
9. Gorenflo, R., Mainardi, F., Moretti, D., Paradisi, P.: Time fractional diffusion: A discrete random walk approach. Nonlinear Dyn. **29**(1), 129–143 (2002)
10. Heydari, M.H.: Wavelets Galerkin method for the fractional subdiffusion equation. J. Comput. Nonlin. Dyn. **11**(6), 061,014 (2016)
11. Hosseini, S.M., Ghaffari, R.: Polynomial and nonpolynomial spline methods for fractional sub-diffusion equations. Appl. Math. Model. **38**(14), 3554–3566 (2014)
12. Huang, C.B., Yu, X.J., Wang, C., Li, Z.Z., An, N.: A numerical method based on fully discrete direct discontinuous Galerkin method for the time fractional diffusion equation. Appl. Math. Comput. **264**, 483–492 (2015)
13. Izadkhah, M.M., Saberi-Nadjafi, J.: Gegenbauer spectral method for time-fractional convection-diffusion equations with variable coefficients. Math. Method Appl. Sci. **38**(15), 3183–3194 (2015)
14. Ji, C.C., Sun, Z.Z.: A high-order compact finite difference scheme for the fractional sub-diffusion equation. J. Sci. Comput. **64**(3), 959–985 (2015)
15. Jiang, Y.J., Ma, J.T.: High-order finite element methods for time-fractional partial differential equations. J. Comput. Appl. Math. **235**(11), 3285–3290 (2011)
16. Jin, B.T., Lazarov, R., Zhou, Z.: Error estimates for a semidiscrete finite element method for fractional order parabolic equations. SIAM J. Numer. Anal. **51**(1), 445–466 (2013)
17. Kilbas, A.A., Srivastava, H.M., Trujillo, J.J.: Theory and Applications of Fractional Differential Equations. Elsevier B. V., Amsterdam (2006)
18. Lin, Y.M., Xu, C.J.: Finite difference/spectral approximations for the time-fractional diffusion equation. J. Comput. Phys. **225**(2), 1533–1552 (2007)
19. Liu, Q., Gu, Y.T., Zhuang, P., Liu, F., Nie, Y.F.: An implicit RBF meshless approach for time fractional diffusion equations. Comput. Mech. **48**(1), 1–12 (2011)
20. Luo, W.H., Huang, T.Z., Wu, G.C., Gu, X.M.: Quadratic spline collocation method for the time fractional subdiffusion equation. Appl. Math. Comput. **276**, 252–265 (2016)
21. Ma, Y.B., Sun, C.P., Haake, D.A., Churchill, B.M., Ho, C.M.: A high-order alternating direction implicit method for the unsteady convection-dominated diffusion problem. Int. J. Numer. Meth. Fl. **70**(6), 703–712 (2012)
22. Mainardi, F.: Fractals and Fractional Calculus Continuum Mechanics. Springer, Verlag (1997)
23. Murillo, J.Q., Yuste, S.B.: On three explicit difference schemes for fractional diffusion and diffusion-wave equations. Phys. Scripta **T136**, 014,025 (2009)
24. Nazir, T., Abbas, M., Ismail, A.I.M., Majid, A.A., Rashid, A.: The numerical solution of advection-diffusion problems using new cubic trigonometric B-splines approach. Appl. Math. Model. **40**(7-8), 4586–4611 (2016)
25. Noye, B.J., Tan, H.H.: Finite difference methods for solving the two-dimensional advection-diffusion equation. Int. J. Numer. Meth. Fl. **9**(1), 75–98 (1989)
26. Pirkhedri, A., Javadi, H.H.S.: Solving the time-fractional diffusion equation via Sinc-Haar collocation method. Appl. Math. Comput. **257**, 317–326 (2015)
27. Podlubny, I.: Fractional Differential Equations. Academic Press, London (1999)
28. Razminia, K., Razminia, A., Baleanu, D.: Investigation of the fractional diffusion equation based on generalized integral quadrature technique. Appl. Math. Model. **39**(1), 86–98 (2015)
29. Saadatmandi, A., Dehghan, M., Azizi, M.R.: The Sinc-Legendre collocation method for a class of fractional convection-diffusion equations with variable coefficients. Commu. Nonlinear Sci. Numer. Simul. **17**(11), 4125–4136 (2012)
30. Sayevand, K., Yazdani, A., Arjang, F.: Cubic B-spline collocation method and its application for anomalous fractional diffusion equations in transport dynamic systems. J. Vib. Control **22**(9), 2173–2186 (2016)
31. Shen, W.S., Zhang, C.J., Zhang, J.: Relaxation method for unsteady convection-diffusion equations. Comput. Math. Appl. **61**(4), 908–920 (2011)
32. Shirzadi, A., Ling, L., Abbasbandy, S.: Meshless simulations of the two-dimensional fractional-time convection-diffusion-reaction equations. Eng. Anal. Bound. Ele. **36**(11), 1522–1527 (2012)
33. Shlesinger, M.F., West, B.J., Klafter, J.: Lévy dynamics of enhanced diffusion: Application to turbulence. Phys. Rev. Lett. **58**(11), 1100–1103 (1987)
34. Shu, C., Richards, B.E.: Application of generalized differential quadrature to solve two-dimensional incompressible Navier-Stokes equations. Int. J. Numer. Meth. Fl. **15**(7), 791–798 (1992)
35. Uddin, M., Haq, S.: RBFs approximation method for time fractional partial differential equations. Commu. Nonlinear Sci. Numer. Simul. **16**(11), 4208–4214 (2011)
36. Walz, G.: Identities for trigonometric B-splines with an application to curve design. BIT **37**(1), 189–201 (1997)
37. Yang, X.H., Zhang, H.X., Xu, D.: Orthogonal spline collocation method for the two-dimensional fractional sub-diffusion equation. J. Comput. Phys. **256**, 824–837 (2014)
38. Zaslavsky, G.M., Stevens, D., Weitzner, H.: Self-similar transport in incomplete chaos. Phys. Rev. E. **48**(3), 1683–1694 (1993)
39. Zeng, F.H., Li, C.P., Liu, F.W., Turner, I.: The use of finite difference/element approaches for solving the time-fractional subdiffusion equation. SIAM J. Sci. Comput. **35**(6), A2976–A3000 (2013)
40. Zhai, S.Y., Feng, X.L.: A block-centered finite-difference method for the time-fractional diffusion equation on nonuniform grids. Numer. Heat. Tr. B-Fund. **69**(3), 217–233 (2016)
41. Zhou, F.Y., Xu, X.Y.: The third kind Chebyshev wavelets collocation method for solving the time-fractional convection diffusion equations with variable coefficients. Appl. Math. Comput. **280**, 11–29 (2016)
42. Zhuang, P.H., Liu, F.W.: Implicit difference approximation for the time fractional diffusion equation. J. Appl. Math. & Computing **22**(3), 87–99 (2006)